Completing Fragmentary River Networks via Induced Terrain

Tsz-Yam Lau and W. Randolph Franklin

ABSTRACT: Fragmentary river segments have to be reconnected before addressing various routing and tracking problems. Elevation determines drainage directions, so the partial heights available through LiDAR may provide useful hints on how the segments should be joined. However, it is not trivial how this information can be applied. This paper bridges this gap by proposing the induced structure approach, which first approximates a terrain compatible with those observations, and then derives a river network from that induced terrain. Since the network is derived from an induced terrain that honors the partial observations, we expect that the derived river network will enforce most restrictions imposed by the partial observations. This paper also provides specifics on the implementation. In the first step regarding terrain reconstruction, we find that the optimal scheme depends on the height sample distribution. If the samples are sparsely yet evenly distributed, natural neighbor interpolation with stream burning (NN-SB) is the most cost-effective. If the samples are offered only at the given river locations, the hydrology-aware version of Over determined Palladian Partial Differential Equation (HA-ODETLAP) should be used instead. In the second step concerning river derivation, we find it necessary to favor those given river locations. Otherwise they will be missed out. We set their respective initial water amounts to the critical accumulation level to ensure a river flows across them. In the subsequent branch thinning process, those locations are protected from being trimmed. We foresee applications of our solution framework in a few 2D and 3D network tracing problems with similar observation distribution, like dendrite network reconstruction.

KEYWORDS: LiDAR, river networks, terrain modeling, network tracing

Introduction

Knowledge of complete river networks is essential to a number of geographical and environmental applications, like designing shortest routes for ships, locating forthcoming affected areas of flooding and pollutant leaks, and identifying possible migrations of aquatic organisms. However, that information is usually not immediately available with conventional airborne surveying techniques like standard photogrammetric and multi/hyper-spectral imaging. Clouds and tree canopies often occlude parts of the river network (Asante and Maidment 1999), leaving us disconnected river segments. We may perform ground surveys as supplements, but they are much more costly. Worse still, sometimes we cannot afford the long time they take, or we simply cannot do them due to harsh ground conditions, as in emergency surveys during or immediately after natural disasters like earthquakes, hurricanes and flooding. This leads to a need to connect the broken segments together to form a complete river network. That complete river network usually consists of a number of tree branching structures. Every river location is expected to have a single way for the water to flow out to a terrain edge or a sink within the terrain (Asante and Maidment 1999; Arge et. al. 2003a). The width of the river branches may be large, but very often we aim at the respective "central lines" where water accumulation is a maximum among its immediate neighbors except the one towards which its water flows.

Intuitively, if we have the fragmentary river observations only but not anything else, the best thing that we can do is to join the segments together as if they are typical line pieces (Asante and Maidment 1999). If the gaps are as small as a few pixels wide, we may use the dilation morphological operation to extend the line pieces gradually until their ends meet (Noble 1996). When we want to conserve the collinearity of the segments, the Hough transform (Hough 1962) provides a voting process to make sure that only collinear pixels can be extended. For curves of arbitrary shapes, we may adopt a more complicated technique like the axis-oriented linking (Zhang 2000). Note that they are all assuming line behaviors that we generalize from typical river segments, like shortest routes and segment curvature preservation, in the reconnection process. However, if we also know the set of ground elevations in addition, we may eliminate any possibilities that violate the height constraint, namely that water flows from a higher location to a lower location. This potentially improves the realism of the reconnection results, as

Tsz-Yam Lau and W. Randolph Franklin, Department of Computer Science, Rensselaer Polytechnic Institute, Troy NY 12180, USA. Email: <laut@cs.rpi.edu>, <wrf@ecse.rpi.edu>.
DOI: 10.1559/15230406382162

we are using information that directly affects drainage. As a critical example, suppose that a hill is sitting in between two river segments. Then even though the end points of these two segments are very close, it is highly likely that the flow from one segment does not go to the other one.

To date, Light Detection and Ranging (LiDAR) provides the most promising survey results on ground elevations. It works by emitting laser pulse energy from a plane travelling across a terrain and collecting the backscatters from the ground. The time elapse between a laser pulse emission and the return of the corresponding backscatter tells the distance between the ground and the plane. Together with a georeferenced record on where those pulses are emitted, we can derive the elevation field of the terrain. However, cloud and canopy covers continue to be the major obstacles. The laser cannot pass through the clouds (National Oceanic and Atmospheric Administration Coastal Services Center 2008). For canopies, LiDAR may "see through" the forest as long as we can detect sufficient backscatters of the small footprint laser pulses that propagate through small canopy openings to the ground. If we fail, we may overestimate the ground heights as we identify no data points that are from the ground, or we mistreat the reflections from an above-ground object as true ground backscatters. The critical coverage extent that still allows enough reflections depends on vegetation type. For instance, in a recent extensive ground survey on a closed-canopy forest in Oregon, it is found that once the canopy cover is over 60%, the ground height estimation degrades quickly. At areas with 90% canopy coverage, the error can be as high as 4 meters for conifers and 3 meters for hardwood during leaf-on seasons (Gatziolis et. al. 2010). These errors can be critical if we are working with a flat area, in which a small noise in the elevation grid can alter the drainage directions and hence impact the resulting derived river network significantly. To obtain reliable ground data of the forest, it is advised to survey in a clear winter night, when clouds are as few as possible, and the leaf-off conditions of the trees could provide more holes in between the canopies for the laser pulses to penetrate (UK Forest Commission 2010).

In summary, the additional elevation data is also likely to be unreliable for some parts of the terrain and hence incomplete. We identify the following two possible sample height distributions:

Case 1. Vegetation cover is not that dense overall (as in typical forest areas). We end up with sparsely and evenly distributed height samples.

Case 2. Vegetation cover is so dense that there is no way for the laser beam to penetrate all the way to the ground. We end up with height values at only the observed river locations where trees cannot grow to block the view of both airborne hydrology and height surveys.

This article aims to introduce a novel conceptual framework for the challenging river segment

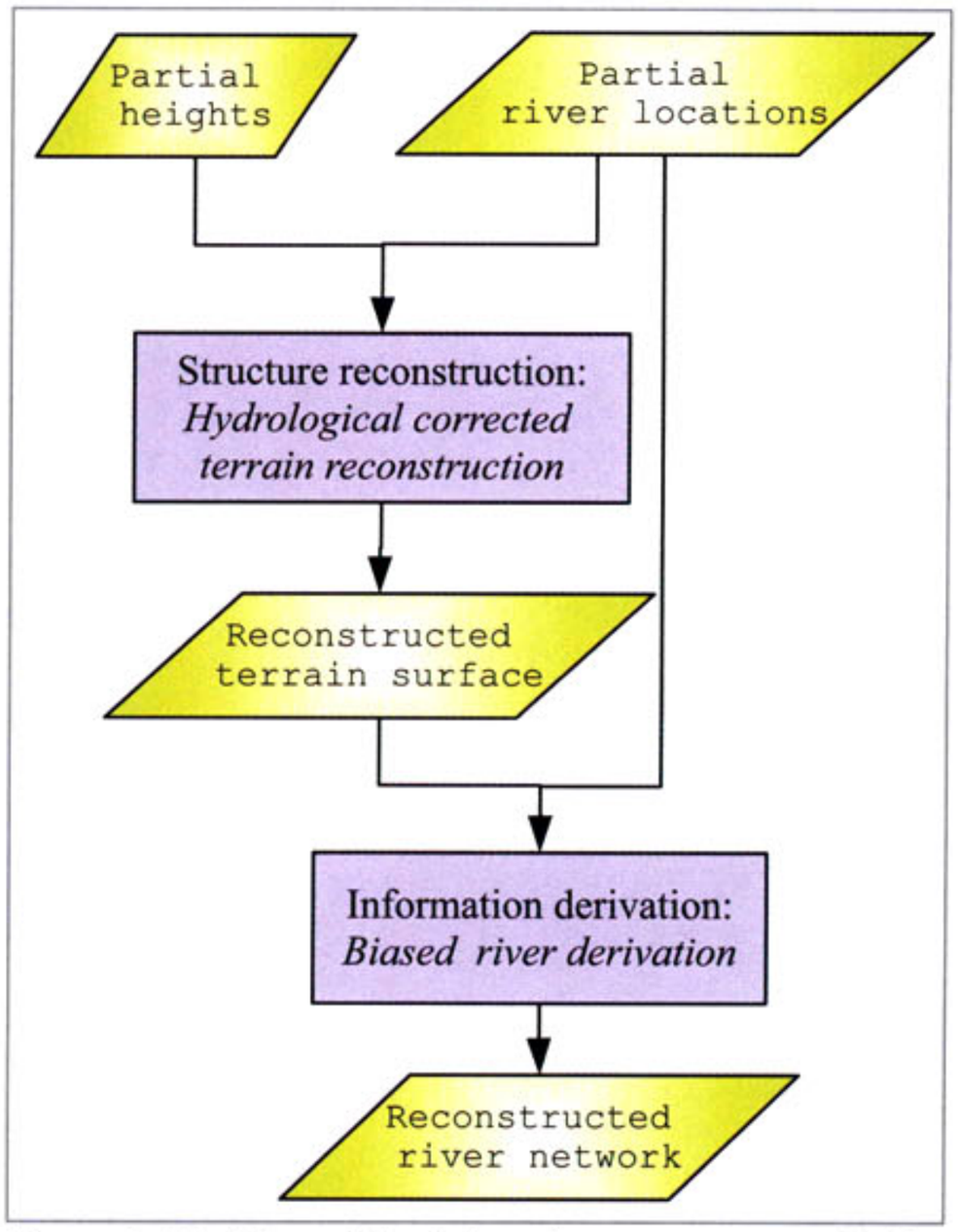

Figure 1. Workflow of the induced structure approach of river network reconstruction.

reconnection problem under the partial height constraint. We call it the induced structure approach. Its workflow is illustrated in Figure 1. The approach incorporates height data by first approximating a structure (a terrain surface in this case) that is compatible with both partial height and river locations information, and then deriving the river network underlying the induced terrain. Since the network is derived from an induced terrain that honors the partial observations, we expect that the derived river network will enforce most restrictions imposed by the partial observations, including the drainage restrictions imposed by the known heights and an exact match of the river locations against the given information. Note that the two steps defined above have been well studied for decades. This means existing well-established algorithms may be applied. What we need to do is to find out the best one, and modify them to adapt to the specific situations we have here.

In this article we will first go through a few concepts related to our discussion, including problem formulation, terrain reconstruction, hydrological correction, river network derivation, and sample datasets. Next we will discuss the first step of the approach, and suggest the best strategies for reconstructing legal terrains under the sample height distributions identified above. We may fail to identify some already given partial river locations if the induced terrain in the previous step is passed to a conventional river derivation algorithm. To eliminate such failures, we privilege those locations throughout

the subsequent river derivation process and provide details of this process. We conclude with suggestions for future research.

Related Concepts

Problem Formulation

In this river segment reconnection problem, the primary data is a square grid of resolution $n \times n$ gridding the terrain in concern. Each of these n^2 cells has a binary value indicating if it is on a river. We have the reconnection problem because we fail to survey a few cells due to dense cloud and tree canopy covers. Some of these cells may be river locations, but we do not flag them as so in that binary data grid. Our task is to find out those cells and flag them back to river locations, so as to obtain the complete river network.

As discussed before, we have also the digital elevation model (DEM), which is the digital representation of the terrain height values. We can always assign it the same resolution as the previous binary grid. Again, this grid may not be completely filled due to dense cloud and canopy covers.

Terrain Reconstruction

If the full DEM grid had been available, the corresponding complete river network would have been readily derivable using a river derivation algorithm as discussed in the subsequent *River Derivation* section of this article. However, holes are now there in the elevation grid. We have to complete the missing values by a terrain reconstruction algorithm before proceeding to the subsequent hydrological correction and river derivation because both processes work only with a complete elevation grid.

Nearly all terrain reconstruction algorithms follow this first law of geography: everything is related to everything else, but near things are more related than distant things (Tobler 1970). Essentially they set the elevation of an unknown position (i, j), $z_{i,j}$, to be a weighted average of known elevations h_l where $l = 1, 2, \ldots, k$:

$$z_{i,j} = \sum_{l=0}^{k} w_{(i,j),l} h_l$$

Proximity polygon (or Voronoi polygon or nearest point) sets $z_{i,j}$ to its nearest known neighbor, which means $w_{(i,j),l} = 1$ for the nearest known position but $w_{(i,j),l} = 0$ for all the others (Thiessen 1911). Because the one neighbor to use for elevation estimation has been clearly defined, it requires no parameters and is therefore simple. However, the surface so generated is blocky because the value used as the interpolated height changes abruptly when crossing the Voronoi boundaries of the known elevations.

Incorporating multiple known heights in the calculation allows their influences to transit smoothly across the terrain, and is a way to improve the surface realism. Inverse distance weighting (IDW) sets $w_{(i,j),l}$ to the inverse power of distance between (i, j) and the known position l, usually square (Shepard 1968). Kriging is a geostatistical approach in which all control point data are involved in finding optimal values of the general weighting function $w(s)$ for a known point distant s from the unknown position. The main assumption here is that the covariance between two elevations depends solely on the distance between the positions (Krige 1951). However, we often have problems optimizing the number of points to use. We would prefer a scheme that takes multiple known heights yet requires no parameter input.

Natural neighbor interpolation (NN) (Sibson 1981) is a representative example of such a scheme. The set of neighboring known heights together with their respective weights are well-governed by Voronoi diagrams. Figure 2, which is adopted from Wikipedia (Wikipedia 2010), illustrates this method. The black

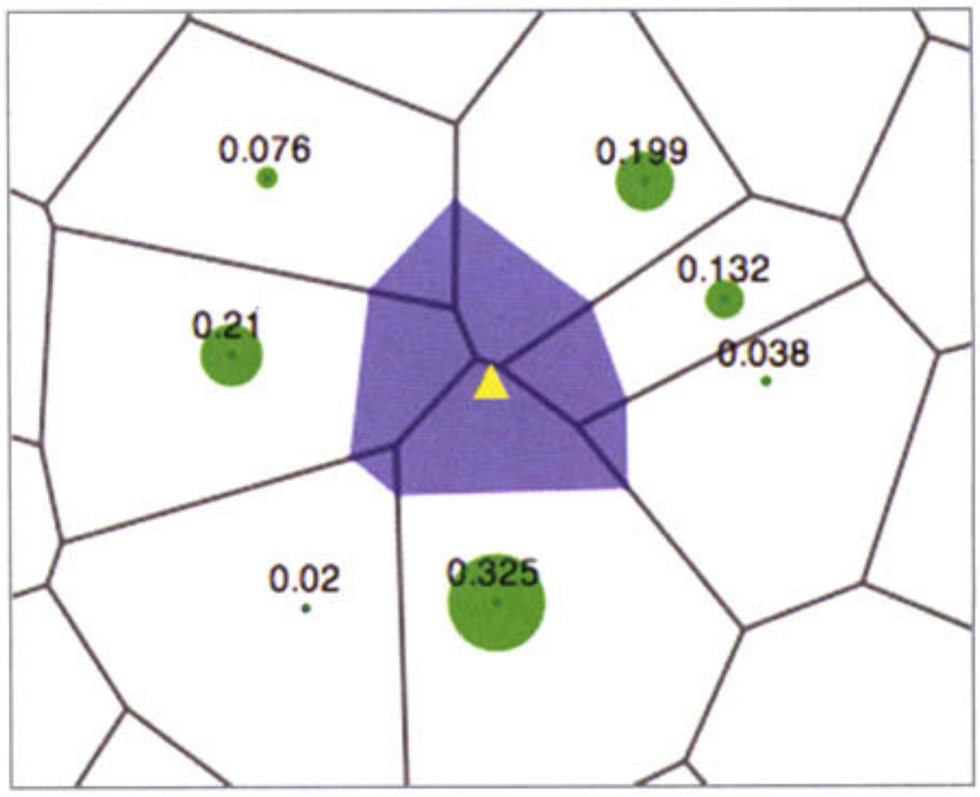

Figure 2. Natural neighbor interpolation.

dots are the locations of the given height samples. The process starts with constructing a Voronoi diagram with these height samples. (The thick solid lines are the boundaries of the Voronoi polygons.) For a unknown-height location p (indicated with a triangle), we identify the corresponding closest subset by first adding p to the Voronoi diagram formed previously, and then find the set of points with their respective original Voronoi polygons overlapping with the Voronoi polygon of p. The interpolated value of p is then the weighted sum of the height values at these closest height samples, with weights proportional to the overlapped area of the Voronoi polygons.

Another parameter-less method involves fitting splines in between the known heights. With this approach, first-order and even second-order continuity are explicitly enforced; thereby ensuring that the slope of the surface is smooth.

In all the approaches described above, we take the measured elevation values as is for the reconstructed surface, also known as interpolation. However, in most cases such interpolation of the known points is not necessary because of measurement imprecision.

Approximation, which allows relaxation from the measured values, allows much more desirable overall reconstruction results and much smoother surfaces.

Trend surface analysis is a classic technique used for surface approximation. It involves specifying a general form of a mathematical function at the beginning. This is the trend which is expected to represent a large-scale systematic change that extends from one map edge to the other. Then we fit the function with the sample data aiming least squares, a process also known as regression. A review of the technique can be found from Wren (1973). However, to model complicated surfaces, we should accompany this approach with some other techniques.

Overdetermined Laplacian Partial Differential Equation (ODETLAP) (Gousie and Franklin 1998; Gousie and Franklin 2005; Xie et. al. 2007) sets up an overdetermined system $\mathbf{Az} = \mathbf{b}$, as shown in Figure 3, to solve for the elevations of the whole terrain grid $\mathbf{z}$. The system includes an exact equation for each known-height position. That equation sets the height value of the respective position to its known value. The system also contains an averaging equation for every position. The equation attempts to regularize the respective height to the average of its immediate four neighbors. Through adjusting the weight R of the set of exact equations over the set of averaging equations, we obtain terrain surfaces with the desired accuracy-smoothness tradeoff. It can work with contour lines (continuous or intermittently broken), infer mountain tops inside a ring of contours, and enforce continuity of slope across contours. All these are favorable features of natural-looking terrains. The time complexity of ODETLAP is $O(n^3+k)$. In practice, we transform the system to $\mathbf{A^TAz} = \mathbf{A^Tb}$ before solving for $\mathbf{z}$. In this equivalent system $\mathbf{A'z} = \mathbf{b'}$ where $\mathbf{A'} = \mathbf{A^TA}$ and $\mathbf{b'} = \mathbf{A^Tb}$, $\mathbf{A'}$ is symmetric positive definite. We can then take advantage of the fast Cholesky factorization to keep the actual solving time to within seconds even for large datasets (Li 2010).

Hydrological Correction Schemes

All the above general terrain reconstruction techniques work primarily with partial height grids. To incorporate the known river locations in the induced terrain, a few hydrological correction schemes have been developed. These schemes are originally intended for full DEMs accompanied with the respective full river networks. They all aim to improve the ability of the DEMs in replicating hydrological patterns, especially in flat landscapes in which noise in heights can harm the river implied by the terrain drastically. The common tactic of many such correction schemes is to sink the elevations of the identified river locations. The simplest is to trench only those river locations by a certain trench amount, a process commonly known as stream burning (Hutchinson 1989). We expect the lowered positions are more likely to see water stop there, thus increasing their chance of becoming river locations. Indeed this matches with our expectation on the height of a river location relative to the corresponding riverbank. Some algorithms suggest sinking the neighborhoods as well, but they require more parameter inputs. For instance, in AGREE (Hellweger 1997) which is available as a script in ArcGIS Arc Macro Language (AML) format, we need to decide the sink width w. We trench the river locations and their neighborhoods by different amounts (sharpdist and smoothdist respectively).

The remaining schemes bundle terrain reconstruction and hydrology adaptation together as integrated hydrology-aware terrain construction algorithms. The best known is ANUDEM (Hutchinson 1989), in which iterative finite difference interpolation is interleaved with the drainage enforcement algorithm. The enforcement algorithm creates not only valleys at the river locations but also chains of decreasing elevations along the flow pathways to guide the water flow. Even without the stream network, the routine can still infer drainage lines via flow directions or even just partial elevations (through an analysis of grid points and saddle points). This practice potentially gives better terrain reconstruction results. However, this also means we need to recompute the whole elevation grid when data are updated, because now there is a tight topological relationship between consecutive locations along the river.

River Network Derivation

To derive the underlying river network of a complete elevation grid, we use a river derivation algorithm like `r.watershed` which is a routine in GRASS GIS (Ehlschlaeger 2008), or TERRAFLOW (Arge et. al.,2003a) which is available as a standalone program (Toma 2002), a routine called `r.terraflow` in GRASS GIS (Arge et. al. 2002) and an extension for ArcGIS (Arge et. al. 2003b). In such an algorithm, we first compute the drainage directions of the cells. Then based on those drainage directions and the initial water amounts assigned to the cells, we evaluate the total amount of water passing through each cell. Finally, the river network compatible with the terrain can be extracted by excluding those positions with accumulation less than a certain threshold.

These different schemes differ in the way they compute drainage directions. For example, in the large-dataset-optimized TERRAFLOW, we rely on typical single-flow direction approaches like the D-8 algorithm (or its 4-neighbor version D-4) in which water is directed to the lowest deeper immediate neighbor (O'Callaghan and Mark 1984), or multiple-flow direction schemes in which water is allowed to flow to multiple neighbors as long as they are deeper. In either case, we need to remove the false local depressions due to noise before computing the drainage directions. Otherwise, water in those depressions cannot be routed to the terrain edges as desired. Common approaches for this task include median filtering (which is well-known in image

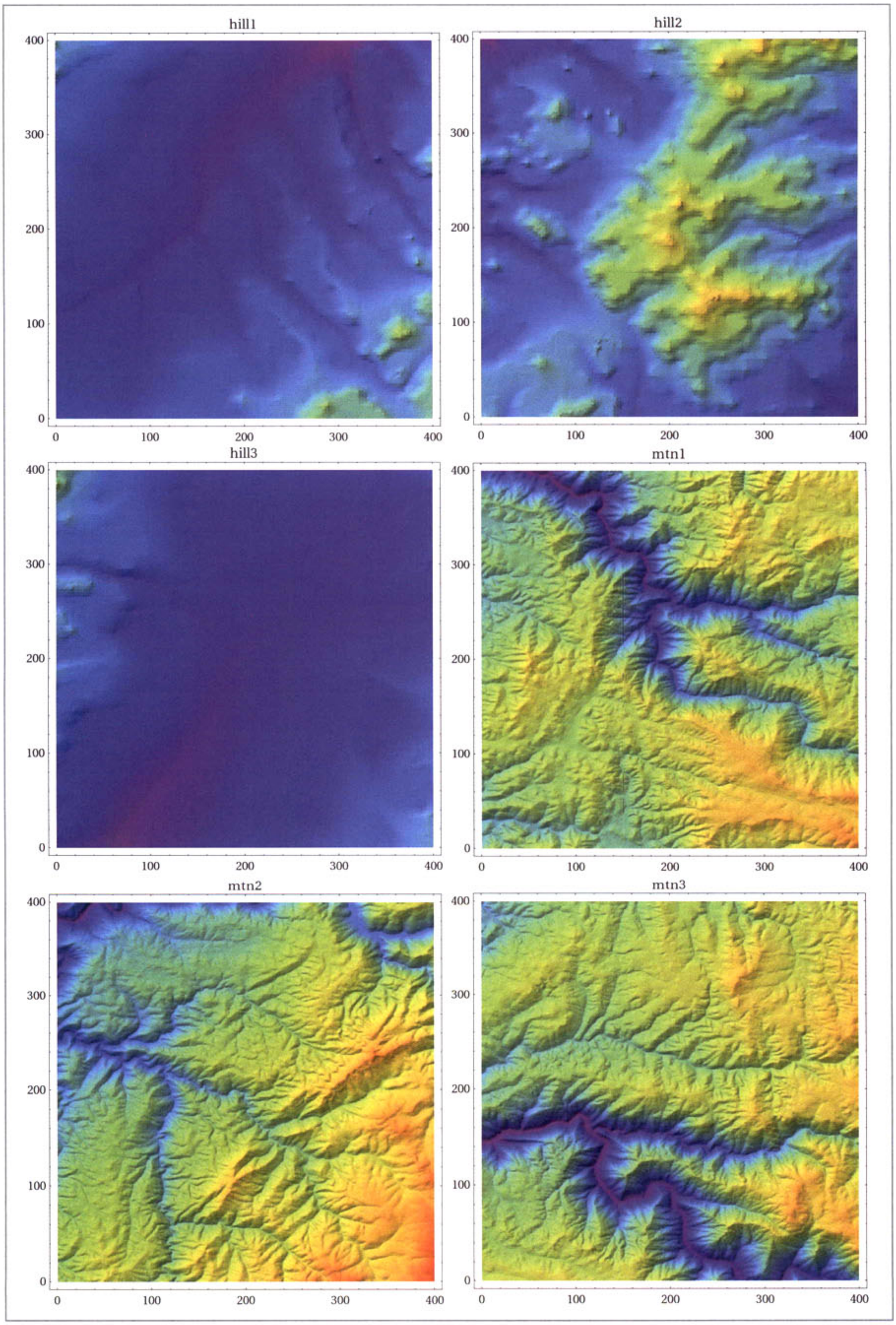

Figure 4. Elevation plots of the six test 400×400 DEMs: *hill1*, *hill2* (first row), *hill3*, *mtn1* (second row), *mtn2*, *mtn3* (third row).

processing literature for suppressing one-cell sinks) and flooding (Arge et. al. 2003a) (which mimics the natural way to assign uphill flow directions to route water out of a sink). An exception is `r.watershed` which uses a least-cost search algorithm. With this algorithm, the drainage of a cell is not determined until its downstream location has been decided, so false pits will not cause drainage flow pointers to go askew. This implies that the single water flow direction can be to some other deeper neighbor which may not be the lowest (Ehlschlaeger 1989). This approach is reported to produce more accurate results in areas of low slope as well as DEMs constructed with techniques that mistake canopy tops as the ground elevation (Ehlschlaeger 2008).

The one-cell thick and no-loop constraints, if needed, can be enforced by a thinning algorithm (Lam et. al 1992) afterwards. The process successively removes pixels at the outer layers of the object, while retaining any pixel whose removal would alter the connectivity or shorten the legs of the skeleton (Jang and Chin 1990). A typical thinning result should be unbiased: the kept pixels are located at the geographical center of the object.

Sample Datasets

In the following discussion, we are using the six 400 × 400 full DEMs shown in Figure 4. Those DEMs are extracted from two SRTM DTED Level 2 cells, with details given in Table 1 and Figure 5. We start with complete elevation data because we need the complete and accurate ground truth river networks for comparison with the reconnection results. Real partial observations rely on humans to complete the missing parts which may means errors.

Table 1. Information about the six test 400×400 DEMs.

DEM	Cell Name	Cell Range	Elevation (m)		
			Mean	Standard Deviation	Range
hill1	W111N31	401:800, 1:400	1251	79	1105:1610
hill2	W111N31	401:800, 401:800	1548	134	1198:1943
hill3	W111N31	401:800, 801:1200	1309	59	1199:1699
mtn1	W121N38	1201:1600, 1201:1600	712	146	219:1040
mtn2	W121N38	280:3200, 801:1200	847	152	330:1283
mtn3	W121N38	3201:3600, 401:800	723	161	233:1021

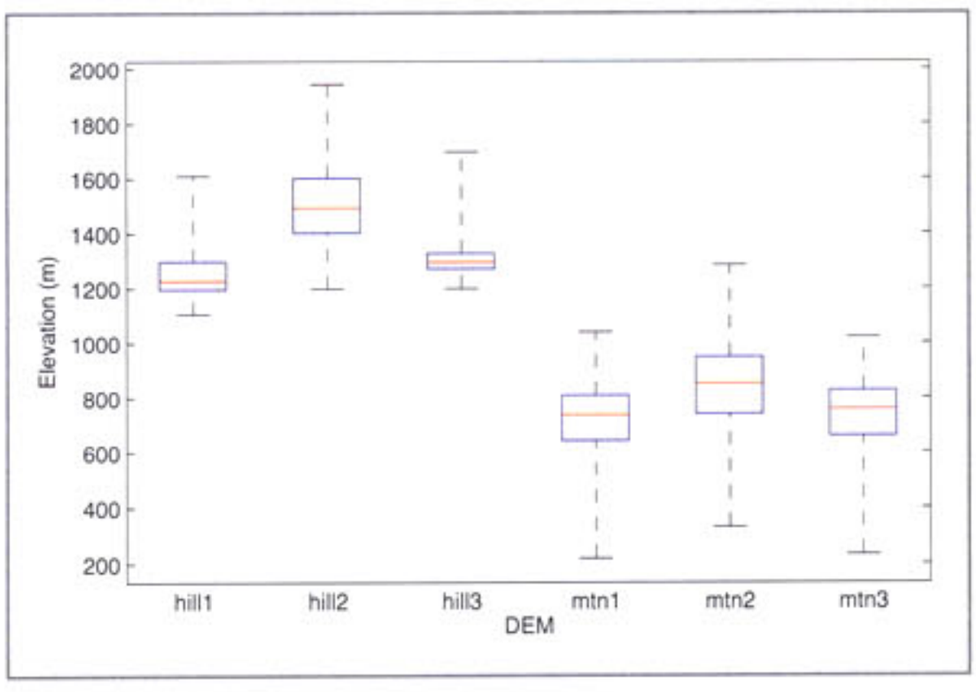

Figure 5. The box plots on the elevations of the six test 400×400 DEMs. For each dataset, the red horizontal bar inside the box indicates the median. The lower and upper sides of each boxes show the 25th and 75th percentiles. The horizontal lines at the lower and upper ends highlight the minimum and maximum.

To obtain the ground-truth river networks, we run `r.watershed` with accumulation cutoff threshold = 200, initial water amount at each location = 1 over these six DEMs. We pick `r.watershed` due to its speed and accuracy over TERRAFLOW. We arbitrarily choose to obtain four-connected river networks.

We sample for observed river locations as follows: first we divide the whole grid into 20 × 20 subgrids. In each subgrid, we randomly pick a point and mask an area of 12 × 12 around it. It is to mimic the occlusions by clouds in real aerial photos. For elevation grid, we hide around 90% of the height values in the elevation grid to simulate the even yet moderate occlusions by clouds and canopies in case 1. For case 2, we hide the heights at all locations except those at the given river locations in order to emulate the effect of severe ground vegetation covers.

Hydrological-corrected Terrain Reconstruction

The first step of the induced structure approach is to derive a terrain compatible with the partial observations. As seen in the previous section, a plethora of terrain reconstruction and hydrological correction schemes is around. What we need to do is to identify the one scheme that works the best with the particular partial observations that we have. We find that the choice depends heavily on how the height samples are distributed. In the following, we will go through the two possible height distributions identified at the start of this article, and justify the respective hydrological-corrected terrain reconstruction schemes that we have chosen.

Evaluation Criteria

To evaluate the various schemes, we pass the partial heights and river locations to various hydrological-corrected terrain reconstruction algorithms to

generate the respective induced terrains, from which we derive the respective river networks using the biased river derivation scheme.

Accuracy is, as always, an important concern when making the decision. In this case, it is evaluated in terms of how well the derived river network links the river segments and classifies the locations as river/non-river. For the former criterion, we provide the plots of the reconstructed networks together with the original one for visual comparison. For the latter, we compute the rates that the reconstructed terrains correctly classify a location as a river/non-river site.

When accuracies are similar, we will turn to efficiency. This implies that we should aim at a scheme that has the smallest number of effective parameters (preferably none at all). This is because to compute the new river network of the updated terrain, we have to work with the whole completed elevation grid, as a river originating at a location can reach virtually any location in the grid no matter how far away it is. Therefore, unless we have a universal parameter setting that is highly likely to yield satisfactory results, we need to go through the global river derivation operation again and again to find out the optimal parameter values, which time and resources may not allow. The errors consist of false positives and false negatives. A false positive occurs when a location has no river flow but is misidentified as a river location. A false negative happens when the river does flow across the location, but the location is misidentified as a non-river location in the reconstructed network.

Case 1: Heights Sparsely Yet Evenly Distributed Across the Terrain

We start working on this case by trying numerous possible combinations of terrain reconstruction and hydrological correction schemes. Table 2 describes those combinations in detail.

The full and the given river networks of mtn1 are given in Figure 6. Figure 7 shows the reconnections with different algorithms. Indeed, it is hard to tell from the figures which scheme is better. First, the results do not show any obvious artifacts. Second, each approach features its own set of correct reconnections.

Table 3. Case 1 - River/Non-river classification errors with respect to all locations of different algorithms. Inside each cell is the classification error, in percentage of cells being misidentified. The parameters needed for the optimal results are in parentheses.

DEM	NN-SB	SF-SB	OS-SB	NN-AGREE	ANUDEM
hill1	1.94	2.38	1.76 (R=1)	2.00 (w=2)	4.17
hill2	2.14	2.17	1.93 (R=10)	2.11 (w=2)	3.76
hill3	3.19	4.54	3.46 (R=5)	3.28 (w=2)	6.45
mtn1	2.48	2.88	2.47 (R=20)	2.44 (w=5)	3.82
mtn2	2.42	2.53	1.90 (R=20)	2.29 (w=5)	3.43

For example, while ANUDEM correctly reconnects the river segments as highlighted by the circle in the middle, it fails for those surrounded by another circle on the right. This means we should turn to the remaining evaluation criteria, namely river/non-river classification errors (shown in Table 3) and efficiency.

Among all the general terrain reconstruction

Table 2. Case 1 - Various hydrological corrected reconstruction schemes being tested.

Scheme	Terrain Reconstruction	Hydrological Correction	Remarks
NN-SB	Natural Neighbor	Stream Burning (trench = 30)	Our recommended scheme. Trench amount is arbitrary set.
SF-SB	Second-order Spline Fitting	Stream Burning (trench = 30)	Reference. It is to investigate if some other parameter-less general terrain reconstruction scheme (Second-order spline fitting) performs better.
OS-SB	ODETLAP (optimal R)	Stream Burning (trench = 30)	Reference. It is to see how much better a more sophisticated general terrain reconstruction scheme (ODETLAP) can perform. We vary R from among 1, 2, 5, 10 and 20, and pick the setting that leads to the smallest false negative with respective to the given river locations.
NN-AGREE	Natural Neighbor	AGREE (sharpdist = 30, smoothdist = 30, optimal w)	Reference. It is to check how better a more complicated hydrological correction scheme can perform. We vary w from among 1 (which is equivalent to stream burning), 2, 5 and 10, and pick the one that gives smallest false negative with respective to the given river locations.
ANUDEM	Finite-difference Interpolation	Drainage Enforcement	Reference. It is to examine whether that existing integrated algorithm that is originally designed for use with full river networks also works well with partial river segments. We use the implementation named TOPOGRID in ARCGIS 9.3. To compare fairly with NN-SB which requires virtually no adjustment of parameters, we do not alter any of its default parameter settings.

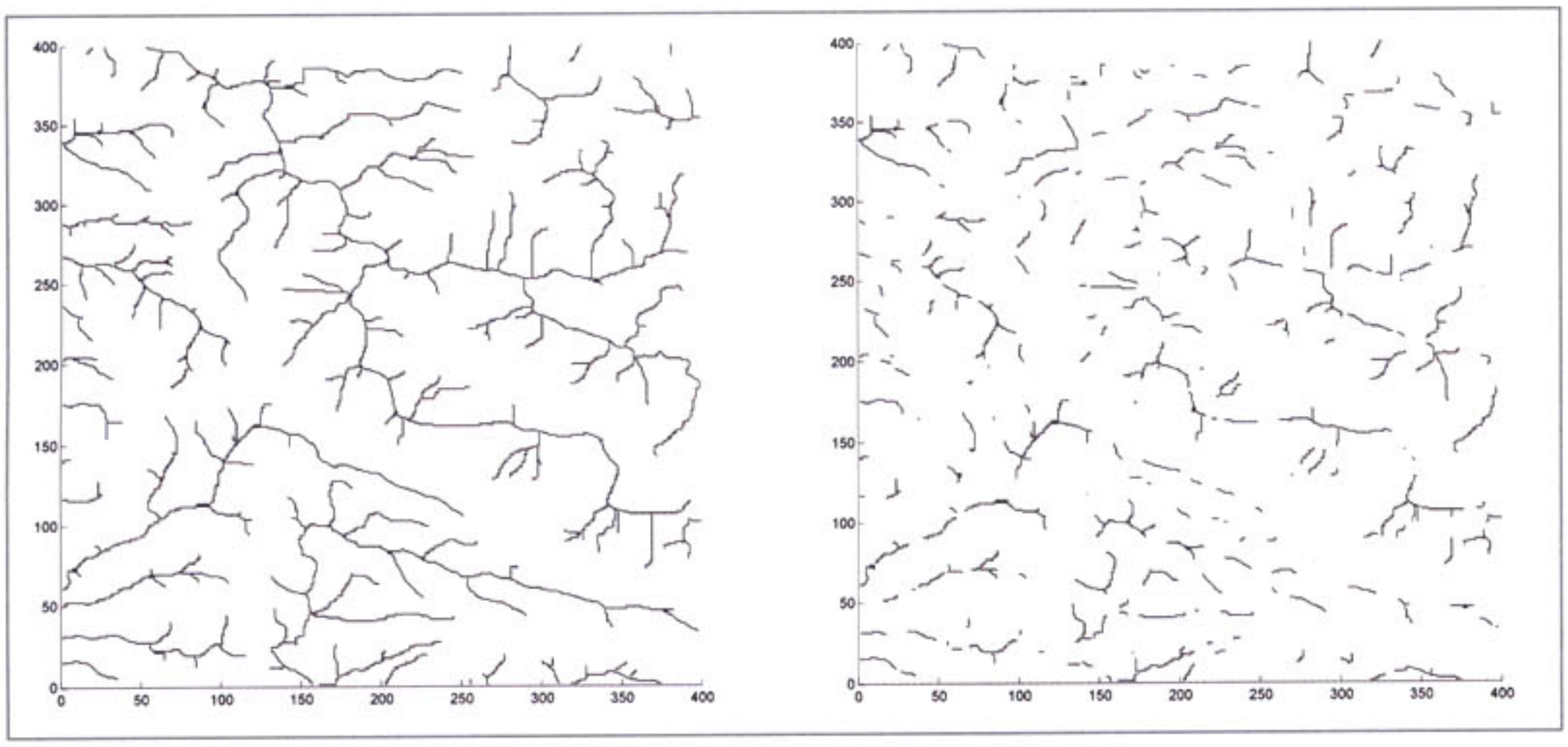

Figure 6. The full river network of mtn1 (left). The given partial river network (right).

Figure 7. Case 1 - The full river network (top left). Reconstructed river networks with different algorithms, NN-SB (top right), SF-SB (middle left), OS-SB (middle right), NN-AGREE (bottom left), ANUDEM (bottom right).

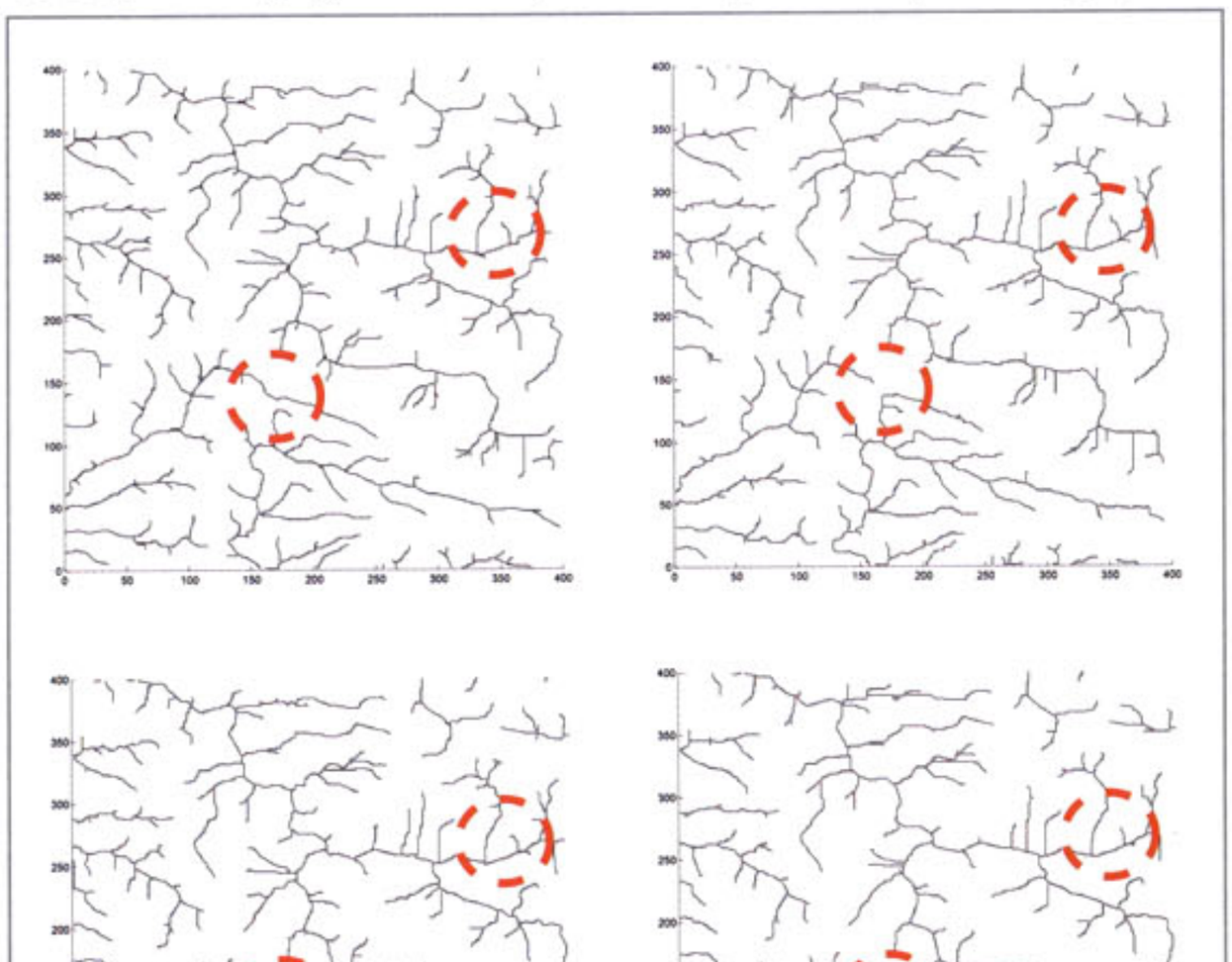

algorithms, natural neighbor interpolation is the only known algorithm to-date that offers reasonably delicate results without any supply of parameter: when comparing within the virtually parameter-less schemes, NN-SB consistently presents smaller errors than SF-SB. This means natural neighbor picks neighbors and sets respective weights better than spline fitting; when compared with OS-SB which requires parameter inputs, NN-SB occasionally performs a little bit more poorly. This is not surprising as ODETLAP which reconstructs terrain for OS-SB is known to have a few advantages in building natural-looking terrains. However, the expense is that we have to run the global river derivation algorithms again and again for the optimal parameter settings, as there is no one-size-fit-all parameter value for different datasets (note the different optimal R values for different DEMs in Table 2). Considering that accuracy improvement is usually within 1 percentage point, we recommend the more efficient natural neighbor.

For the hydrological correction strategy, we adopt stream burning over the more complicated AGREE. The arguments are similar to that for natural neighbor over ODETLAP: first, even though stream burning takes trench amount as the only parameter, the strategy is virtually parameter-less. Its effect is there as long as the amount is large enough. Further fine-tuning on the parameter does not change the result much (Callow et. al. 2007). In contrast, we need to adjust *sink width w* for AGREE (note the different optimal *w*

value in for different DEMs in Table 2); second, we gain at most 1 percentage point in accuracy, if there is any (compare the errors of NN-SB with NN-AGREE in Table 2). Indeed, setting $w = 1$ (which is equivalent to NN-SB) sometimes offers superior results (See *hill1* and *hill3*). All these justify our choice on the more cost-efficient stream burning.

The integrated hydrology-aware terrain reconstruction algorithm ANUDEM does not perform equally well as NN-SB. We suspect the reason is that the topological relationship buildup that it features to improve accuracy does not work well with broken river segments.

Case 2: Height available at given river locations only

We once again try all the possible (terrain reconstruction, hydrological correction) combinations as in case 1 to look for the best one. In this case, we find that the hydrology-aware variant of Overdetermined Laplacian Partial Differential Equation (HA-ODETLAP) gives the most accurate river/non-river classification, especially at the tributaries. These locations are where other conventional schemes depend heavily on given height samples to infer ridges and valleys crucial to correct water distribution and river formation.

Recall the key idea of a hydrological corrected terrain reconstruction scheme is to model river locations as local minima with respect to surrounding non-river locations. To realize this idea in HA-ODETLAP, we modify the averaging equation at each known river location: we regularize its height

$$z_{i,j} = \frac{z_{i-1,j} + z_{i+1,j} + z_{i,j-1} + z_{i,j+1}}{4} - d$$

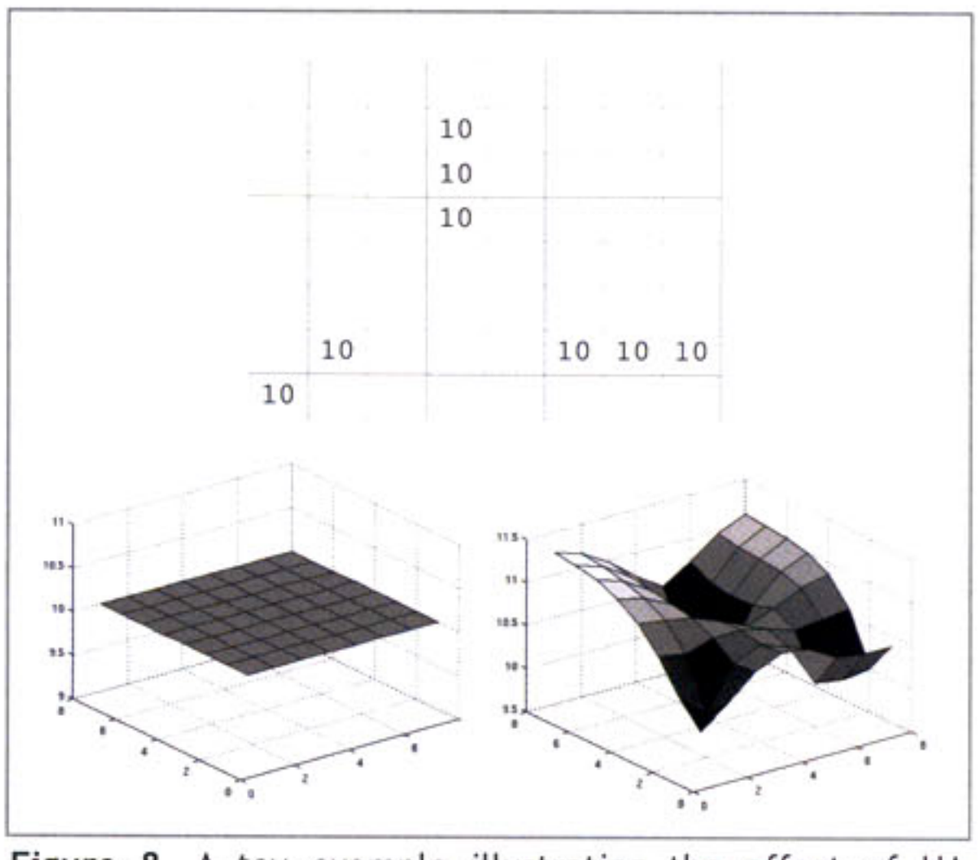

Figure 8. A toy example illustrating the effect of HA-ODETLAP. Known river locations with respective heights (top). Terrain reconstructed using basic ODETLAP (bottom left). Terrain reconstructed using HA-ODETLAP with f = 1.04 (bottom right).

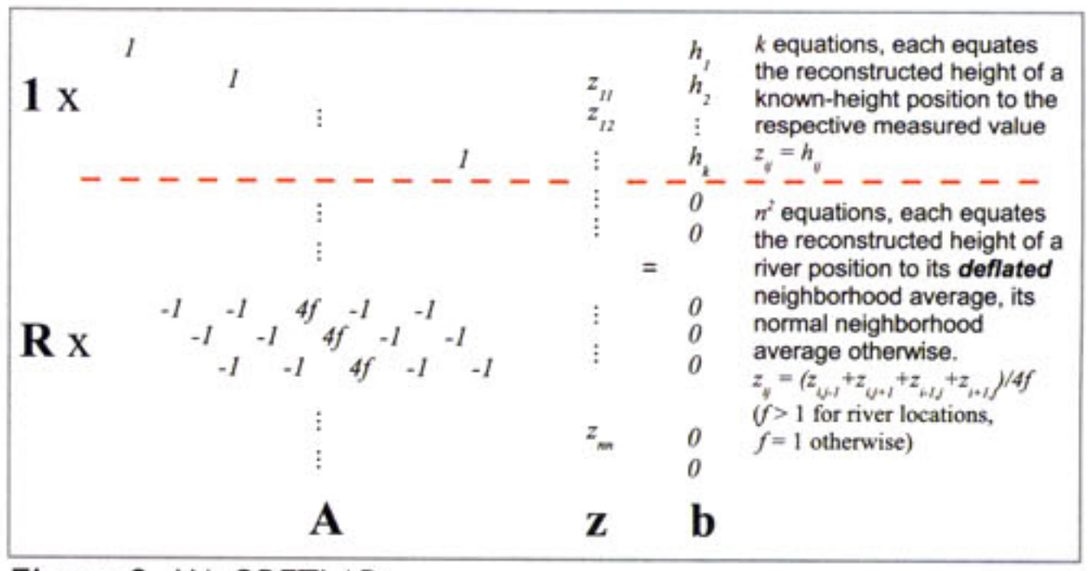

Figure 9. HA-ODETLAP.

to a value smaller than the respective neighborhood average.

If we assume that the slope of the river bank is approximately the same throughout the whole terrain (as in flat basins), we deduct those neighborhood averages by the same amount d (Muckell 2008).

$$z_{i,j} = \frac{z_{i-1,j} + z_{i+1,j} + z_{i,j-1} + z_{i,j+1}}{4f}$$

Otherwise, it is more appropriate to deflate the average more at higher elevations. It is because youthful river channels, which are usually located at high elevations and also the beginning of a river, have steeper slopes than the mature and old age counterparts at lower elevations (GeoTeach.com 2008).

The f above is the average deflation factor: if we increase its value from 1, the value imposed to $z_{i,j}$ by this averaging equation decreases from the neighborhood average. With sufficiently large f, that value will be smaller than any of its non-river immediate neighbors. The computed surface will then have a local minimum at that location. Figure 8 illustrates how HA-ODETLAP makes a difference. The regularization part of ODETLAP attempts to set the height value of every cell to the average of its immediate four neighbors. Therefore, when it is confronted with an incomplete height grid in which all the given elevations are of the same (10 in this case), that single elevation value is propagated to all the unknown height cells, resulting in an undesirable flat surface. In contrast, with HA-ODETLAP under $f > 1$, the regularization equation at each known-height river location models the location as a local minimum instead, resulting in the desirable "V" shape there.

Figure 9 summarizes the overall system of our hydrology-aware extension. When compared with Figure 3, one can see that we only change the values of some non-zero entries in the A matrix. Zero locations in the original system remain zeros. The sparsity structure of the A matrix is preserved. Thus the modified system can be solved within a time similar to the original system.

As in the original system, the accuracy-smoothness parameter R determines the trade-off between smoothness of the reconstructed terrain and

Table 4. Case 2 - River/Non-river classification errors of HA-ODETLAP under different average deflation factors f, together with NN-SB (trench = 30). Inside each cell is the classification error, in percentage of cells being misidentified.

DEM	HA-ODETLAP with *f*					NN-SB
	1.00	1.01	1.02	1.03	1.04	
hill1	6.15	2.60	2.67	2.73	2.72	3.18
hill2	6.75	2.41	2.51	2.56	2.58	3.78
hill3	6.52	3.50	3.50	3.51	3.54	3.43
mtn1	6.89	2.59	2.50	2.45	2.45	4.20
mtn2	6.86	2.73	2.71	2.64	2.62	4.42
mtn3	6.17	2.77	2.64	2.69	2.71	4.14

accuracy of the known heights. Here since all the height samples are concentrated at the river locations, terrain surface smoothness is not that relevant, and this justifies a high accuracy setting, say $R = 20$. The new parameter f is much more interesting and thus worth more attention.

Table 4 shows how f matters. $f = 1.00$ is equivalent to the original implementation. At that setting, HA-ODETLAP performs worse than NN-SB (which we find the best for case 1) because HA-ODETLAP at that setting is essentially the same as conventional ODETLAP. ODETLAP does not model the given river locations as local minima. For all other settings, we see significant improvements over NN-SB. Indeed, we find that for this particular set of terrains, $f = 1.02$ gives consistently satisfactory results in general.

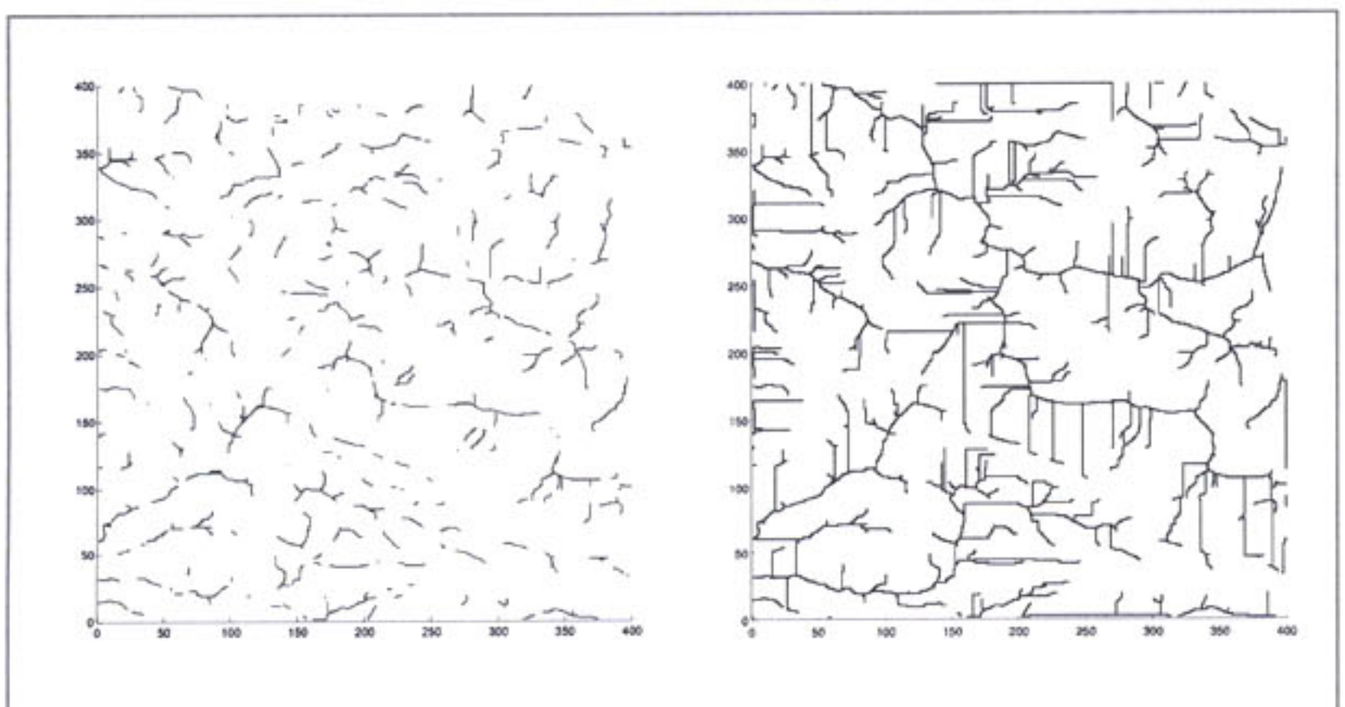

Figure 10. Case 2 - Available partial river segments, and hence locations with measured heights (top left). NN-SB river reconstruction result (top right). Hydrology-aware ODETLAP result with $f = 1.02$ (bottom).

Figure 10, top left, shows the partial river locations and heights we offer, and its top right and bottom show the recovered river connections using these two terrain reconstruction schemes. One can immediately realize that the tributaries cannot be correctly reproduced when NN-SB is used: in this case we do not have any height sample in the non-river area. As a result, NN-SB fails to reconstruct the proper "V"-shape centered at the river lines across the non-river regions, which is important for deducing proper tributaries. In contrast, the hydrology-aware adaptation in ODETLAP infers local minima as long as the corresponding locations are defined to be river locations, regardless of whether heights are available.

Biased River Derivation

Note that in the above discussion, we emphasize the use of a biased river derivation algorithm rather than a typical river derivation algorithm. It is necessary because the typical procedure fails to reproduce every identified river location. Figure 11, top right, highlights those identified river locations that fail to show up in the reconstructed river network (with mtn1 as the underlying terrain dataset). The biased procedure aims to eliminate this situation within the river derivation procedure. In the following, we will discuss two biasing schemes and their rationales.

Biased Initial Water Assignment

A major source of such false negatives is the set of the side streams which mark the onset of rivers. They fail to be parts of the river network again because insufficient water gets through them in the reconstructed terrain. As the terrain is already the best that we can reconstruct, we attempt to enable river flow across those locations in a different way: recall that we identify a location as a river location as long as water accumulation there exceeds a certain threshold value. Therefore, by assigning every known river location an initial water amount that is equal to that critical value, they are automatically made river locations even if no water flows into them. Note that this practice does not harm their downstream locations, as we know water should come out from those already-known river locations anyway. In fact it helps to recover those river locations that are downstream of those given river locations.

Such a change does not incur much additional work to the river derivation algorithm. For example, with r.watershed, one is ready

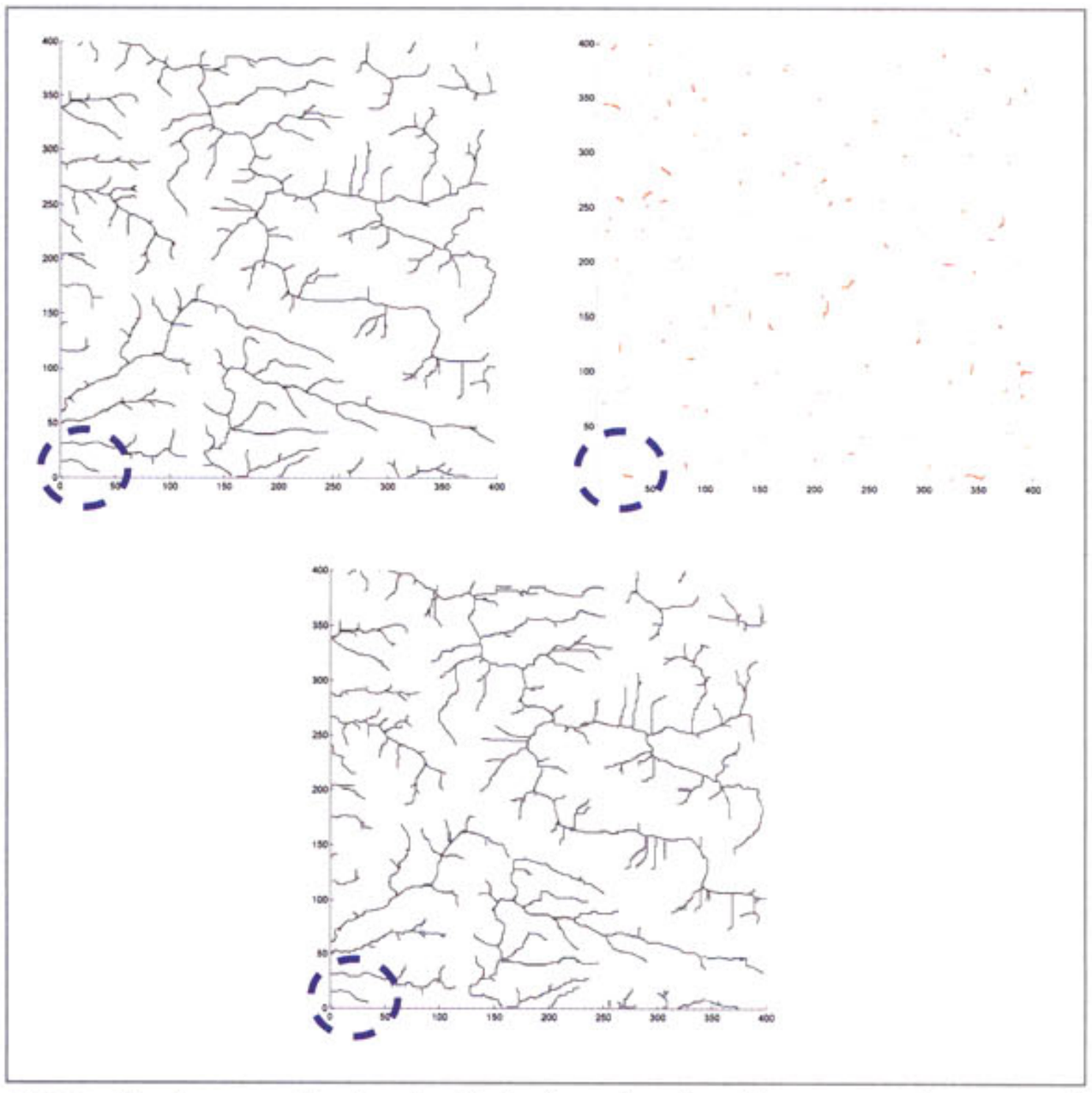

Figure 11. An example showing that given river locations may not recovered with conventional unbiased river derivation scheme. The full river (top left). The river network reconstructed using a conventional unbiased river derivation scheme is highlighted in light grey, while those given river locations being missed out are marked in dark red (top right). The river network derived by our biased river derivation scheme (bottom).

to specify the initial water amounts of individual locations as a matrix parameter.

Biased thinning

Another source of false negatives comes from those river locations not lying on exactly the geographical center of the preliminary river. Recall from our previous discussion that the result of typical thinning is unbiased: the kept pixels are located at the geographical center of the object. If that algorithm is applied to the preliminary biased river network above, we may lose a few given river cells because of the inconsistency between the geographical center and the "center line" of a river segment. We expect that the "center line" of a thick preliminary river segment consists of its local-minimum locations, where water accumulations are at local maximum. Those locations may not be located exactly at the geographical center of the river segment.

To fix this problem, we impose an additional constraint on the thinning procedure: we disallow removal of all the known river locations. We privilege those identified river locations when deciding whether to keep the cells or not in the thinning process. Such a small change does not introduce too much overhead. We adapt a mask-based thinning algorithm (Diaz de Leon et. al. 2004) for biased thinning in our prototype. The gain in running time is insignificant.

Evaluation

The bottom diagram of Figure 11 shows the river derivation results of *mtn1* using the above biasing techniques, and Table 5 presents the respective river/non-river classification errors. As expected, all the given river locations are identified correctly, as shown in the diagrams that all river locations marked in red in the top right diagram are recovered in the bottom figure, and in the table as the drop in false negatives with respect to given river locations. This contributes to part of the drop in overall classification errors. An additional benefit is on those non-given river locations which are located downstream of these given river locations. They are also rediscovered because their upstream now has sufficient water to support river flow across them. An example is given in the circled area in the figure. This improvement leads to further drop in the overall classification errors.

Conclusion and Future Work

We have presented the induced structure approach for completing fragmentary river networks. Its main idea is to first reconstruct a structure based on the available partial observations, and then use the induced structure to derive the information we need. Since we are deriving the information from a structure induced according to the partial observations, we expect that the derived information will enforce most restrictions imposed by the observations.

When this concept is applied to fragmentary river network completion, in the structure reconstruction step we delineate a terrain surface that respects the partial height observations, and portray the identified river locations as local minima. In case height samples are sparsely yet evenly distributed across the terrain, we achieve competitive results in terms of

Table 5. River/Non-river classification errors with typical and biased river derivation schemes. The figures outside the parentheses are percentages with respect to all cells. Those inside are percentages with respect to given river locations only.

DEM	Typical	Biased
hill1	1.97 (9.51)	1.77 (0.00)
hill2	2.14 (12.12)	1.89 (0.00)
hill3	3.19 (24.37)	2.82 (0.00)
mtn1	2.48 (10.33)	2.21 (0.00)
mtn2	2.42 (11.35)	2.13 (0.00)
mtn3	2.50 (11.46)	2.25 (0.00)

river location classification with NN-SB. It does not require any parameter adjustment, thus saving us from repeatedly generating the terrain with different parameters and running the global river derivation scheme in order to look for the optimal ones. This feature is especially crucial when we are confronted with increasingly massive terrain datasets. When height samples are available at given river segment locations only, we suggest HA-ODETLAP instead. By regularizing all given river locations as local minima and other locations as the immediate neighborhood average, this approach induces ridges and valleys at not only given river locations but also areas without any height samples properly. We believe that this is the reason why HA-ODETLAP induced-terrains offer superior tributaries and hence smaller river/non-river classification errors.

In the subsequent information derivation process with the biased river derivation scheme, we allocate critical initial amounts of water to the given known river locations, and protecting them from removal during the final thinning process. As a result, we recover not only the entire given river locations but also their connections to the main streams.

The beauty of our work lies in that the two component processes above are both well-studied yet evolving. Once a particular technique used in either field becomes mature, we are ready to adopt it to our work.

Having seen the success of this set of techniques wth completing hydrology networks, we are extending our work by studying the effect of the terrain type (like flat tidal wetlands) on the reconnection results. A particular terrain type may imply a specific pattern on how the underlying rivers look like. Therefore it may affect how the terrain should be induced and how the river network should be formed. We are also eager to port the same solution framework to complete some other 2D networks like road networks, and extend it to solve 3D network completion problems like fragmentary dendrite networks.

ACKNOWLEDGMENTS

This research was partially supported by grant CMMI-0835762 from the National Science Foundation. Work presented in this paper is extended from workshop and conference papers written by the same authors (Lau and Franklin, 2010a, Lau and Franklin, 2010b). We would like to appreciate Prof. Barbara Cutler and a few anonymous reviewers for their critical comments on the content. We would also thank Dr. Barbara Lewis, Mr. Matt Rolph and Ms. Elia Desjardins for their advice on the language.

REFERENCES

Arge, L., J.S Chase, P. Halpin, L. Toma, J.S. Vitter, D. Urban and R. Wickremesinghe. 2003a. Efficient flow computation on massive grid terrain datasets. *Geoinformatica* 7(4): 283–313.

Arge, L., A.B. Danner, L.I. Toma and J. Vahrenhold. 2003b. *The TerraFlow-extension for ArcGIS 8.x.* http://wwwmath1.uni-muenster.de:8010/u/jan/TerraFlowExtension/, (accessed 18 Feb 2011).

Arge, L., H. Mitasova and L. Toma. 2002. *r.terraflow.* http://www.cs.duke.edu/geo*/terraflow/r.terraflow.html, (access 18 Feb 2011).

Asante, K. and D. Maidment. 1999. *Creatng a river network from the arcs in the digital chart of the world.* http://www.ce.utexas.edu/prof/maidment/grad/asante/dcw/rivernet.htm, (accessed 23 2010).

Callow, J.N., K.P.V. Niel and G.S. Boggs. 2007. How does modifying a DEM to reflect known hydrology affect subsequent terrain analysis? *Journal of Hydrology* 332: 30–39.

Diaz de Leon, J.L., C. Yanez and G. Giovanni. 2004. Thinning algorithm to generate k-connected skeletons. In: A. Sanfeliu, J.F. Martinez Trinidad and J.A. Carrasco Ochoa (eds.), *Progress in Pattern Recognition, Image Analysis and Applications, Lecture Notes in Computer Science*, v.3287, Springer Berlin-Heidelberg, pp. 115–135.

Ehlschlaeger, C. 1989. Using the AT search algorithm to develop hydrologic models from digital elevation data. In: *Proceedings of the International Geographic Information System (IGIS) Symposium*, pp. 275–281.

Ehlschlaeger, C. 2008. *GRASS GIS: r.watershed.* http://grass.itc.it/gdp/html_grass63/r.watershed.html, (accessed 23 Jun 2010).

Gatziolis, D., J.S. Fried and V.S. Monleon. 2010. Challenges to estimating tree height via LiDAR in closed-canopy forests: A parable from western Oregon. *Forest Science* 56(2): 139–155.

Geoteach.com, 2008. *Classifying rivers - three stages of river development.* http://www.geolor.com/geoteach/Online/Three_Stages_of_River_Development-geoteach.pdf, (accessed 17 Feb 2011).

Gousie, M. and W.R. Franklin. 1998. Converting elevation contours to a grid. In: *Eighth International Symposium on Spatial Data Handling*, Dept of Geography, Simon Fraser University, Burnaby, BC, Canada, Vancouver BC Canada, pp. 647–656.

Gousie, M.B. and W.R. Franklin. 2005. Augmenting grid-based contours to improve thin plate DEM generation. *Photogrammetric Engineering & Remote Sensing* 71(1): 69–79.

Hellweger, R. 1997. *Agree.aml.* Center for Research in Water Resource, The University of Texas at Astin, Austin, TX.

Hough P.V.C. 1962. *Method and Means for Recognizing Complex Patterns.* US Patent 3069654.

Hutchinson, M.F. 1989. A new procedure for gridding elevation and stream line data with automatic removal of spurious pits. *Journal of Hydrology* 106: 211–232.

Jang, B. and R. Chin. 1990. Analysis of thinning algorithms using mathematical morphology. IEEE *Transactions on Pattern Analysis and Machine Intelligence* 12: 541–551.

Krige, D.G. 1951. *A statistical approach to some mine valuations and allied problems at the Witwatersrand.*

Master's thesis, University of Witwatersrand.
Lam, L., S. Lee and C. Suen. 1992. Thinning methodologies - a comprehensive survey. *IEEE Transactions on Pattern Analysis and Machine Intelligence* 14: 869–885.
Lau, T.-Y. and W.R. Franklin. 2010a. Completing fragmentary river networks via induced terrain. In: *Geospatial Data and Geovisualization: Environment, Security, and Society, a special joint symposium of ISPRS Technical Commission IV & AutoCarto 2010, American Society for Photogrammetry and Remote Sensing*, Orlando, Florida.
Lau, T.-Y. and W.R. Franklin. 2010b. Completing river networks with only partial river observations via hydrology-aware ODETLAP. In: *20th Annual Fall Workshop on Computational Geometry* (FWCG 2010), Stony Brook University, Stony Brook, NY 11794, USA. (extended abstract and talk).
Li, Y., T.Y. Lau, C.S. Stuetzle, P. Fox and W.R. Franklin. 2010. 3D oceanographic data compression using 3D-ODETLAP. In: *18th ACM SIGSPATIAL International Conference on Advances in Geographic Information Systems*.
Muckell, J. 2008. *Evaluating and compressing hydrology on simplified terrain*. Master's thesis, Rensselaer Polytechnic Institute.
National Oceanic and Atmospheric Administration Coastal Services Center. 2008. *LiDAR 101: An introduction to LiDAR technology, data, and applications*. http://www.csc.noaa.gov/digitalcoast/data/coastallidar/_pdf/What_is_Lidar.pdf, (accessed 18 Feb 2011).
Noble, J. A. 1996. The effect of morphological filters on texture boundary localization. *IEEE Transactions on Pattern Analysis and Machine Intelligence* 18: 554–561.
O'Callaghan, J.F. and D.M. Mark. 1984. The extraction of drainage networks from digital elevation data. *Computer Vision, Graphics, and Image Processing* 28: 323–344.
Shepard, D. 1968. A two-dimensional interpolation function for irregularly-spaced data. In: *Proceedings of the 1968 ACM National Conference*, pp. 517–524.
Sibson, R. 1981. A brief description of natural neighbor interpolation. In: V. Barnett (ed.), *Interpreting Multivariate Data*, John Wiley & Sons, New York, pp. 21–36.
Thiessen, A. H. 1911. Precipitation averages for large areas. *Monthly Weather Review* 39(7): 1082–1084.
Tobler, W. 1970. A computer movie simulating urban growth in the Detroit region. *Economic Geography* 46(2): 234–240.
Toma, L. 2002. *TerraFlow download*. http://www.cs.duke.edu/geo*/terraflow/download.html, (accessed 18 Feb 2011).
UK Forestry Commission, 2010. *Archaeological prospecting in woodland using LiDAR*. http://www.forestry.gov.uk/fr/INFD-6FKHFE, (accessed 22 Nov 2010).
Wikipedia. 2010. *Natural neighbor*. http://en.wikipedia.org/wiki/Natural_neighbor, (accessed 1 Dec 2010).
Wren, A. E. 1973. Precipitation averages for large areas. *Canadian Journal of Exploration Geophysics* 9(1): 39–44.
Xie, Z., M.A. Andrade, W.R. Franklin, B. Cutler, M. Inanc, D.M. Tracy and J. Muckell. 2007. Approximating terrain with over-determined Laplacian PDEs. In: *17th Fall Workshop on Computational Geometry*, IBM TJ Watson Research Center, Hawthorne NY. poster session, no formal proceedings.
Zhang, Y. 2000. A Method for Continuous Extraction of Multispectrally Classified Urban Rivers. *Photogrammetric Engineering and Remote Sensing* 66(8): 991–1000.